

## Cluster dynamical mean field theory of quantum phases on a honeycomb lattice

Rong-Qiang He and Zhong-Yi Lu\*

*Department of Physics, Renmin University of China, Beijing 100872, China*

(Received 25 December 2011; published 6 July 2012)

We report the cluster dynamical mean field theory calculations performed for the ground state of the half filled Hubbard model on a honeycomb lattice with exact diagonalization on the cluster-impurity solver. Through using elaborate numerical analytic continuation, we identify the existence of a “spin liquid” from the on-site interaction  $U = 0$  to  $U_c$  (between  $4.6t$  and  $4.85t$ ) with a smooth crossover correspondingly from the charge fluctuation dominating phase into the charge correlation dominating phase. The semimetallic state exists only at  $U = 0$ . We further find that the magnetic phase transition at  $U_c$  from the spin liquid to the Néel antiferromagnetic Mott insulating phase is a first-order quantum phase transition. We also show that the charge fluctuation plays a substantial role on keeping the spin liquid phase against the emergence of a magnetic order.

DOI: [10.1103/PhysRevB.86.045105](https://doi.org/10.1103/PhysRevB.86.045105)

PACS number(s): 71.27.+a, 71.30.+h, 71.10.Fd

Quantum phase transition is a fascinating physics subject, which describes an abrupt change of the ground state of a quantum many-body system tuned by a nonthermal physical parameter, often accompanied with a novel quantum emergence phenomenon.<sup>1</sup> As a canonical quantum phase transition, the Mott transition, from the metallic to the insulating state tuned by electronic Coulomb interaction, is one of the most celebrated and difficult problems in condensed-matter physics.<sup>2</sup> The resultant insulating state, namely Mott insulator, usually adopts spontaneous symmetry breaking in two and three spatial dimensions to form a long-range antiferromagnetic (AFM) order to release the spin entropy due to localized electrons. Theoretically, the simplest model to capture such physics is the standard one-band half filled Hubbard model. In the large Coulomb interaction limit this model reduces to a standard Heisenberg model with an AFM order in its ground state.

Nevertheless, an insulating ground state without any spontaneous symmetry breaking, namely spin liquid, may arise if there is frustration.<sup>3,4</sup> Actually spin liquid is a genuine Mott insulating state in a sense that it is adiabatically separated from a band insulator. Spin liquid has been one of the most intriguing issues in condensed-matter physics since it was introduced nearly forty years ago<sup>3</sup> and continuously in intense research since it was further proposed to be a parent phase to likely lead to high- $T_c$  superconductivity.<sup>5</sup> However, a spin liquid had not been verified for a two-dimensional (2D) standard Hubbard or Heisenberg model until a recent quantum Monte Carlo (QMC) simulation was done for the Hubbard model on a honeycomb lattice.<sup>6</sup> Through finite-size extrapolation the simulation shows that a spin liquid emerges between semimetallic and AFM Mott insulating phases with the on-site interaction  $U$  between  $3.5t$  and  $4.3t$ . By contrast, the previous similar QMC simulations only showed a transition from semimetallic to AFM insulating phase around  $4.5t$ .<sup>7</sup> Considering that finite-size calculations, whether QMC simulations or exact diagonalizations (EDs), disallow spontaneous symmetry breaking and have low resolution on spectral functions due to finite-size effects, it is thus in strong demand to employ another complementary approach to further study this fundamental issue, the nature of such a spin liquid phase and the related quantum phase diagram.<sup>8,9</sup>

On the other hand, being complementary to the finite-size calculations, the nonperturbative cluster dynamical mean field

theory (CDMFT) allows spontaneous symmetry breaking and naturally realizes the thermodynamic limit to avoid finite-size effects so that it can uniformly describe the whole coupling regime. Thus, to help to clarify the issue, we adopted the CDMFT to study the half filled Hubbard model on a honeycomb lattice as

$$\hat{H} = -t \sum_{\langle ij \rangle, \sigma} (c_{i\sigma}^\dagger c_{j\sigma} + \text{H.c.}) + U \sum_i n_{i\uparrow} n_{i\downarrow}, \quad (1)$$

where  $c_{i\sigma}^\dagger$  ( $c_{i\sigma}$ ) is the electron creation (annihilation) operator with spin  $\sigma$  ( $\uparrow$  or  $\downarrow$ ) at lattice site  $i$ ,  $\langle ij \rangle$  represents the summation over the nearest neighbors,  $t > 0$  is the nearest-neighbor hopping integral, and  $n_{i\sigma} = c_{i\sigma}^\dagger c_{i\sigma}$  with the on-site Coulomb repulsion  $U$ .

The model (1) had been studied by single-site dynamical mean field theory which did not include spatial correlations,<sup>10</sup> being questionable. To include spatial correlations, two CDMFT studies have recently been done for this model,<sup>9</sup> which show a second-order transition from semimetallic to insulating phase at  $U$  between  $3t$  and  $4t$ . However, neither study considered symmetry breaking, namely AFM order; moreover, they were done in finite temperatures, which degrade the resolution on spectral functions upon ground states.

Our findings are schematically summarized in Fig. 1. We find that a disordered phase of “spin liquid” exists from  $U = 0$  to  $4.6t$ , at which it transforms into the Néel AFM Mott insulating phase via a first-order quantum phase transition. Unlike what is described by the conventional concept on spin liquid, there is large charge fluctuation found in the spin liquid on a honeycomb lattice.

The dynamical mean field theory (DMFT) maps a quantum lattice model onto a single lattice site, a quantum impurity, dynamically coupled to a self-consistently determined bath of free electrons that represents the rest of the lattice.<sup>11</sup> Thus the DMFT fully considers local quantum dynamical fluctuations. This substantially improves our understanding on the nonperturbative properties of correlated electron systems, particularly the Mott transition. The CDMFT is a natural extension of the DMFT to include the missed short-ranged spatial correlations and meanwhile allow spontaneous symmetry breaking through a proper replacement of a single-site impurity by a cluster of

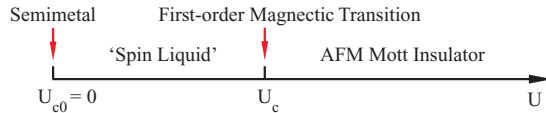


FIG. 1. (Color online) Schematic phase diagram of the one-band Hubbard model on a honeycomb lattice at half filling.  $U_c$  is between  $4.6t$  and  $4.85t$ .

lattice sites, which is constructed to reflect the lattice symmetry and local lattice structure features.<sup>12–14</sup> The CDMFT has been successfully applied to study a variety of ordered phases, and opens an avenue to directly study quantum phase transitions.

Here it should be addressed that for the (C)DMFT the thermodynamic limit is naturally taken from the outset through a self-consistent procedure.<sup>11,14</sup> As a nonperturbative approach to treat many-body correlation effects, the (C)DMFT works well in the whole coupling regime and becomes exact in the two contrary limits of both noninteracting and infinite-interacting cases. For finite-size QMC simulations or EDs, in contrast, the thermodynamic limit is extrapolated through finite-size scaling. Correspondingly, the CDMFT allows spontaneous symmetry breaking, while the finite-size approaches have difficulty in finding a long-range order or underestimate ordered phases. Thus the CDMFT and finite-size approaches are complementary to each other, which together can give more conclusive results than alone.

In CDMFT calculations, the target in the self-consistent procedure is to obtain a lattice imaginary frequency local Green's-function matrix  $G_{ij}(i\omega_n)$  (subscripts  $i$  and  $j$  being site indices of a chosen cluster) by assuming its self-energy matrix identified as the one of the corresponding cluster-impurity Green's-function matrix  $G_{ij}^{imp}(i\omega_n)$ , derived from the Dyson equation. In order to study a ground state, we apply exact diagonalization rather than quantum Monte Carlo simulation to solve a cluster-impurity model.<sup>15,16</sup> Specifically, we employed the robust Krylov-Schur algorithm based SLEPC<sup>17</sup> to accomplish the large-scale sparse matrix diagonalization efficiently and stably.<sup>18</sup> Here we particularly emphasize that to carry out an elaborate numerical analytic continuation from an imaginary frequency Green's function  $G_{ii}(i\omega_n)$  onto a real frequency retarded Green's function  $G_{ii}(\omega + i0^+)$  is crucial to unambiguously identify whether or not an energy gap exists at a small on-site interaction  $U$ ,<sup>19–21</sup> by checking the density of states (DOS) equal to  $-\frac{1}{\pi}\text{Im}G_{ii}(\omega + i0^+)$ . In such a way, the energy gap resolution can be achieved as high as  $10^{-3}t$ , which is hardly reached by other methods.

We first performed the CDMFT calculations for one-dimensional (1D) Hubbard model at half filling with a cluster-impurity model respectively containing two and four lattice impurity sites, which serves as a benchmark for the further calculations. The calculated results are reported in Fig. 2, in quantitative comparison with the Bethe ansatz exact solution.<sup>22</sup> As we see, the two-site CDMFT result has been already in excellent agreement with the exact solution. Especially, by using the numerical analytic continuation, we can unambiguously identify that a finite energy gap immediately develops once  $U$  is nonzero. Thus the short-ranged spatial correlations play a dominant role in local spectral functions and properties even

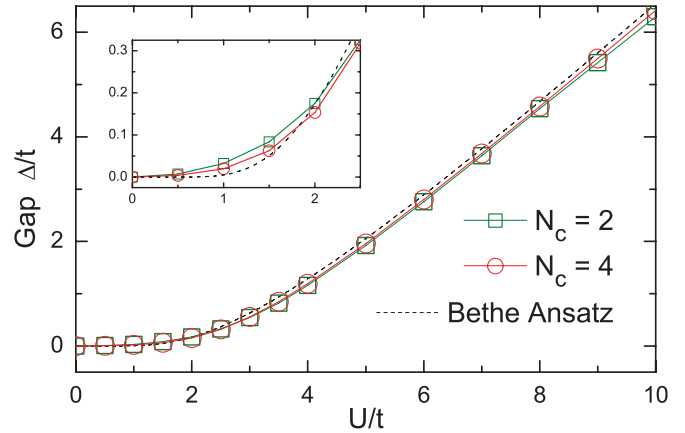


FIG. 2. (Color online) Energy gap  $\Delta$ , namely single-particle spectral gap, as a function of the on-site interaction  $U$  in the one-dimensional half filled Hubbard model, calculated with the two-site ( $N_c = 2$ ) and four-site ( $N_c = 4$ ) clusters, respectively. The dashed curve denotes the exact one from the Bethe ansatz solution. The inset zooms in the small- $U$  dependence.

though the spatial correlations have long-ranged power-law behavior in the 1D Hubbard model.<sup>23</sup> It is also well known that the quantum fluctuations are much stronger in one dimension than in higher dimensions. Hence it is highly expected that the higher dimensional CDMFT results are more reliable and encouraging than the one-dimensional ones.

Figure 3(a) schematically shows the cluster-impurity model constructed for a honeycomb lattice. Such a model reflects sixfold rotational symmetry and an impurity site with a lattice coordination number of 3, which are the essential features of a honeycomb lattice. We also add a direct link between each pair of the nearest bath levels so that we can simulate the propagation of an electron from one cluster site through the outside of the cluster (the bath) to any other cluster site in the calculations.

When the on-site interaction  $U = 0$ , the half filled Hubbard model on a honeycomb lattice reduces to a set of free Dirac fermions with a linear DOS around the Fermi energy. As shown in Fig. 3(b), the numerical analytic continuation can well repeat

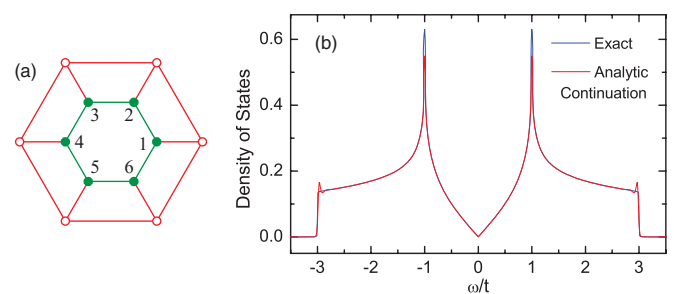


FIG. 3. (Color online) (a) Cluster-impurity model configuration for a honeycomb lattice. Filled circles denote the impurity sites. Unfilled circles denote the bath levels. Links represent the hopping paths. (b) Density of states of the model when  $U = 0$ . The blue curve is the exact one. The red one was obtained by the numerical analytic continuation.

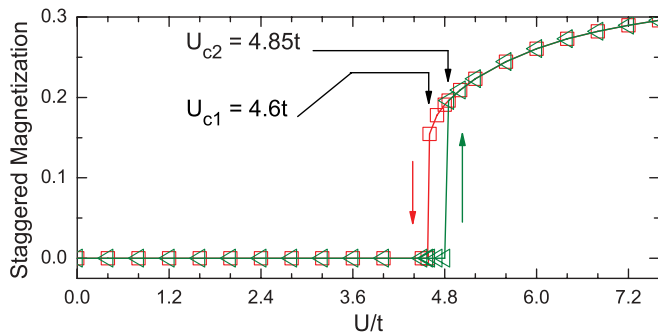


FIG. 4. (Color online) Calculated magnetization as a function of the on-site Coulomb interaction  $U$  on a honeycomb lattice.

the exact DOS. Particularly, around the Fermi energy both are strictly the same even though the DOS is not differentiable at the Fermi energy.

In this study, we define the magnetization  $m = \langle (n_{\uparrow} - n_{\downarrow})/2 \rangle$  on a site. Being bipartite, a honeycomb lattice can be divided into two sublattices  $A$  and  $B$ . If a Néel AFM state appears,  $m$  will alternatively take positive and negative along with sublattices  $A$  and  $B$ , namely being staggered magnetization. As we see from Fig. 4, when  $U < U_{c2} = 4.85t$ , a paramagnetic solution of  $m = 0$  is stable, namely no spin polarization on each site, but over  $U_{c2}$  this solution is no longer stable and  $|m|$  abruptly jumps over 0.2. On the other hand, when  $U > U_{c1} = 4.6t$  a staggered magnetization solution with  $|m| > 0.16$  is stable, namely a Néel AFM phase takes over, but below  $U_{c1}$   $m$  immediately plummets to zero. Between  $U_{c1}$  and  $U_{c2}$ , these two solutions coexist. Such a hysteresis behavior indicates that this magnetic transition is a first-order quantum phase transition.

We calculated the DOS for a small on-site interaction  $U$  with extreme caution through elaborate numerical analytic continuation.<sup>20</sup> The calculated DOSs are then plotted in Fig. 5. Similar to the case of the 1D Hubbard model, what we find is that there is also a definite energy gap opening at the Fermi energy once  $U$  is nonzero. In comparison with the case of  $U = 0$  by checking the enclosed area, it is further shown that the corresponding states nearby the Fermi energy are clearly moved away from the gap rather than pushed to the two sides of the gap. To be specific, for  $U = 0.4t, 0.8t, \text{ and } 1.2t$ , the

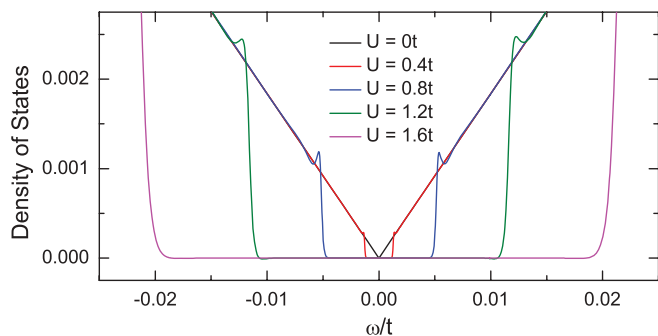


FIG. 5. (Color online) Calculated density of states for several small values of the on-site Coulomb interaction  $U$  on a honeycomb lattice, zooming in around the Fermi energy  $\omega = 0$ .

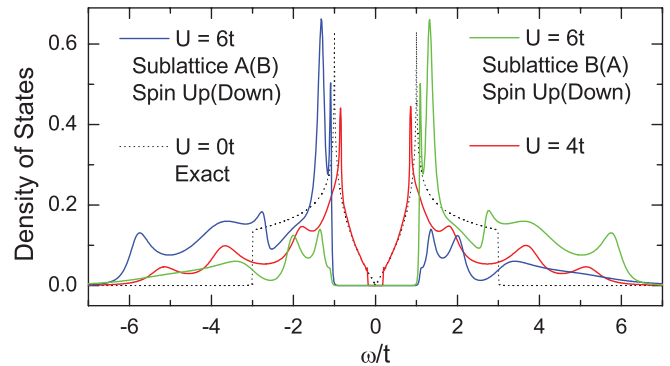


FIG. 6. (Color online) Calculated density of states for  $U = 4t$  (red lines) and  $U = 6t$  (blue and green lines) on a honeycomb lattice, respectively. The dotted curve is the exact DOS at  $U = 0$  for a reference and the Fermi energy sets to zero.

energy gap  $\Delta$  is found to be  $2.5 \times 10^{-3}t, 1.0 \times 10^{-2}t, \text{ and } 0.023t$ , respectively. For a rather large  $U$ , a relatively large energy gap opens with a substantial portion of states moved away from the Fermi energy into below  $-3t$  and above  $3t$ , corresponding to the Hubbard band states. For a  $U$  further larger than  $U_{c2}$ , the system transforms into the Néel AFM phase. The on-site spin degeneracy is then lifted. The spin-up (spin-down) resolved DOS at  $A$  sublattice is the same as the spin-down (spin-up) one at  $B$  sublattice, as shown in Fig. 6.

Figure 7 shows the energy gap  $\Delta$  as a function of the on-site interaction  $U$ , extracted from the calculated DOS. For  $U < 1.6t$ , the energy gap increases very slowly with  $U$ , and the function can be represented as  $\Delta/t = 0.015(U/t)^2$ . After  $1.6t$ , the energy gap increasing becomes fast with  $U$  increasing. Between  $U_{c1}$  and  $U_{c2}$ , the  $U$  dependence of the energy gap shows a hysteresis behavior with a sudden change of  $\sim 0.45t$ , corresponding to the first-order quantum phase transition. Thus a nonzero  $U$  definitely induces an energy gap and makes the system be in an insulating phase. It is noted that for  $U \geq 4t$  the nonmagnetic energy gaps are similar to the ones given by the previous CDMFT calculations,<sup>9</sup> which, however, cannot resolve the small gaps at low  $U$ .

The resulting small- $U$  behavior in the present study is different from the one in the recent QMC aforementioned simulation,<sup>6</sup> and other previous studies based on

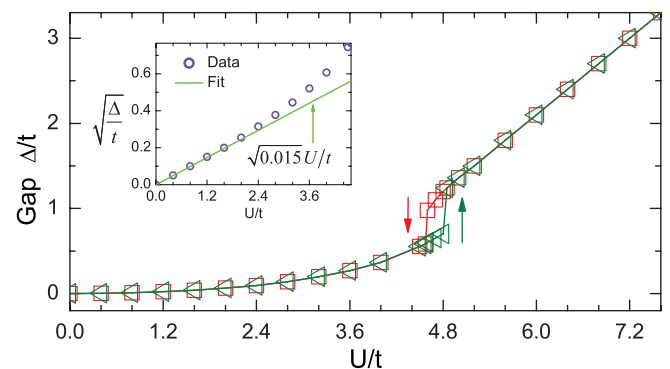


FIG. 7. (Color online) Calculated energy gap  $\Delta$  as a function of the on-site Coulomb interaction  $U$  on a honeycomb lattice. The inset zooms in the small- $U$  dependence.

renormalization-group analysis<sup>24</sup> or  $1/N$  ( $N$  fermion flavors) approximation.<sup>25</sup> Then one may raise a generic question of whether or not in the CDMFT framework a small energy gap will be induced by the missed long-ranged spatial correlations beyond the cluster at a small  $U$ . Accordingly, we have carried out the analogous CDMFT calculations for the 2D triangular Hubbard model, in which the continuous spectrum with a finite value at the Fermi energy at any small  $U$  is well obtained.<sup>26</sup> Nevertheless it should be addressed that the difference on the small- $U$  behavior between the present study and other studies is still an open issue needed to be further explored, considering that the current approaches or methods to deal with a two- or three-dimensional Hubbard model all have their own advantages and drawbacks, usually being complementary to each other.

To explore whether there is a structure to break the honeycomb lattice symmetry and then induce the nonmagnetic energy gaps  $\Delta$ , we need to check different types of correlation functions in site space. We have calculated the equal time spin-spin correlation functions  $\langle s_i^z s_j^z \rangle$  and occupancy-occupancy correlation functions  $\langle n_i n_j \rangle$ , with  $i, j$  inside the cluster-impurity model. We find that all these correlation functions keep the sixfold rotational symmetry before the magnetic transition. This excludes spin valence bond structures, spin anisotropic structures, and charge density waves. Regarding other possible structures, like superconducting state, quantum Hall state, and valence bond crystal, we need to calculate longer range correlation functions, which is beyond the capability of the current CDMFT calculations due to the small-size cluster-impurity model. On the other hand, these structures all have been excluded for  $3.5t < U < 4.3t$  by the recent large-size QMC simulations with lattice sites as large as  $2 \times 18 \times 18$ ,<sup>6</sup> being complementary to the CDMFT calculations. Herewith we can classify the nonmagnetic insulating phase found here from  $U = 0$  to  $U_c$  (between  $4.6t$  and  $4.85t$ ) as a spin-liquid phase in the sense that it is tuned by the on-site interaction  $U$ .

To understand the underlying physics, we examine the double occupancy, defined as  $D = \langle n_\uparrow n_\downarrow \rangle$  on a site. The ground-state energy per site  $E_g = \langle \hat{H} \rangle / N$  of Hamiltonian (1) is a function of the on-site interaction  $U$ . Its derivative is nothing but the double occupancy, namely  $\partial E_g / \partial U = \langle n_\uparrow n_\downarrow \rangle$ . Thus the double occupancy  $D$  directly describes a quantum phase transition tuned by  $U$ . In Fig. 8, the  $U$  dependence of  $D$  likewise shows a hysteresis behavior between  $U_{c1}$  and  $U_{c2}$ . This means that the energy level crossing in the ground state through the magnetic transition as  $U$  increasing, being a characteristic of a first-order quantum phase transition.<sup>1</sup>

The on-site interaction  $U$  tunes or controls the Hamiltonian (1) through the double occupancy  $D$ . Moreover, the localization degree of an electron, as well as the local correlation effect, can be quantitatively described by the double occupancy. At half filling,  $D$  is between 0.25 and 0, corresponding respectively to full delocalization and complete localization. In addition, the magnetic moment  $m_z$  is obtained by  $\langle m_z^2 \rangle = \langle (2S^z)^2 \rangle = 1 - 2D$ .

It is commonly thought that the Mott transition is driven by the strong local correlation effect due to the on-site interaction  $U$ , which is marked by a vanishing or very small double

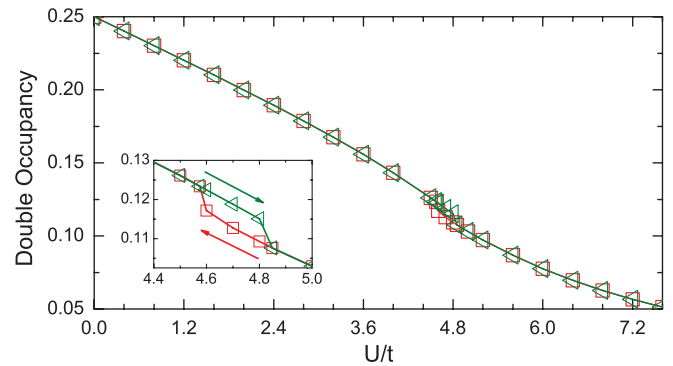


FIG. 8. (Color online) Calculated double occupancy  $D$  as a function of the on-site Coulomb interaction  $U$  on a honeycomb lattice. The inset zooms in the hysteresis loop.

occupancy with a large local moment on a site.<sup>11,27</sup> In contrast, for the Hubbard model on a honeycomb lattice, a small  $U$  can immediately induce a small energy gap opening to tune the system into an insulating phase with a large double occupancy, namely large charge fluctuation, as shown in Fig. 8. It is also noted that the double occupancies before the AFM transition are consistent with the ones given by the previous CDMFT calculations.<sup>9</sup> The calculations further show that the small- $U$  induced energy gap is a consequence of the interplay between the zero DOS at the Fermi energy (Dirac cone band) and local charge correlation, not a conventional correlation-driven Mott insulating gap. On the other hand, the correlation effect will become dominating nearby the magnetic transition  $U_c$ . As shown in Fig. 7, the energy gap becomes a linear function of  $U$  after the transition, which is the canonical behavior of a correlation-driven Mott insulator. The calculated transition  $U_c$  is consistent with those given by the QMC simulations.<sup>6,7</sup> Thus the spin liquid states nearby  $U = 0$  are charge fluctuation dominating while those nearby  $U_c$  are charge correlation dominating, corresponding to the ones derived from the QMC simulation in Ref. 6. Nevertheless our calculations show that a smooth crossover connects these two contrary parts. Meanwhile it is also indicated that the charge fluctuation plays a substantial role on keeping the spin liquid phase against the emergence of an AFM order.

In summary, we have performed the cluster dynamical mean field theory calculations, allowing for the spontaneous symmetry breaking, to study the ground state of the half filled Hubbard model on a honeycomb lattice. We find that a spin liquid exists from  $U = 0$  to about  $4.6t$ , in which the system takes a smooth crossover correspondingly from the charge fluctuation dominating phase into the charge correlation dominating phase, then it further transforms into the Néel antiferromagnetic Mott insulating phase via a first-order quantum phase transition.

We would like to thank N.-H. Tong for very helpful discussions. Z.Y.L. sincerely thanks the hospitality of International Center of Quantum Materials of Peking University, where this paper was finalized. This work was supported by National Natural Science Foundation of China and by National Program for Basic Research of MOST (2011CBA00112), China.



\*zlu@ruc.edu.cn

- <sup>1</sup>*Understanding Quantum Phase Transitions*, edited by L. D. Carr (CRC, Boca Raton, 2011); S. Sachdev, *Quantum Phase Transitions* (Cambridge University Press, Cambridge, England, 2000).
- <sup>2</sup>N. F. Mott and R. Peierls, *Proc. R. Soc. London Ser. A* **49**, 72 (1937); F. Gebhard, *The Mott Metal-Insulator Transition: Models and Methods* (Springer, New York, 1997).
- <sup>3</sup>P. W. Anderson, *Mater. Res. Bull.* **8**, 153 (1973); P. Fazekas and P. W. Anderson, *Philos. Mag.* **30**, 423 (1974).
- <sup>4</sup>L. Balents, *Nature (London)* **464**, 199 (2010).
- <sup>5</sup>P. W. Anderson, *Science* **235**, 1196 (1987).
- <sup>6</sup>Z. Y. Meng, T. C. Lang, S. Wessel, F. F. Assaad, and A. Muramatsu, *Nature (London)* **464**, 847 (2010).
- <sup>7</sup>S. Sorella and E. Tosatti, *Europhys. Lett.* **19**, 699 (1992); T. Paiva, R. T. Scalettar, W. Zheng, R. R. P. Singh, and J. Oitmaa, *Phys. Rev. B* **72**, 085123 (2005).
- <sup>8</sup>F. Wang, *Phys. Rev. B* **82**, 024419 (2010); Y. M. Lu and Y. Ran, *ibid.* **84**, 024420 (2011); B. K. Clark, D. A. Abanin, and S. L. Sondhi, *Phys. Rev. Lett.* **107**, 087204 (2011); C. Xu, *Phys. Rev. B* **83**, 024408 (2011).
- <sup>9</sup>W. Wu, Y.-H. Chen, H.-Sh. Tao, N.-H. Tong, and W.-M. Liu, *Phys. Rev. B* **82**, 245102 (2010); A. Liebsch, *ibid.* **83**, 035113 (2011).
- <sup>10</sup>S. A. Jafari, *Eur. Phys. J. B* **68**, 537 (2009); M. T. Tran and K. Kuroki, *Phys. Rev. B* **79**, 125125 (2009).
- <sup>11</sup>A. Georges, G. Kotliar, W. Krauth, and M. Rozenberg, *Rev. Mod. Phys.* **68**, 13 (1996); G. Kotliar and D. Vollhardt, *Phys. Today* **57**(3), 53 (2004).
- <sup>12</sup>S. Moukouri and M. Jarrell, *Phys. Rev. Lett.* **87**, 167010 (2001).
- <sup>13</sup>G. Kotliar, S. Y. Savrasov, G. Palsson, and G. Biroli, *Phys. Rev. Lett.* **87**, 186401 (2001).
- <sup>14</sup>T. Maier, M. Jarrell, T. Pruschke, and M. Hettler, *Rev. Mod. Phys.* **77**, 1027 (2005).
- <sup>15</sup>M. Caffarel and W. Krauth, *Phys. Rev. Lett.* **72**, 1545 (1994).
- <sup>16</sup>C. A. Perroni, H. Ishida, and A. Liebsch, *Phys. Rev. B* **75**, 045125 (2007).
- <sup>17</sup>V. Hernandez, J. E. Roman, and V. Vidal, *ACM Trans. Math. Softw.* **31**, 351 (2005); J. E. Roman, E. Romero, and A. Tomas, SLEPC home page: <http://www.grycap.upv.es/slepc>, 2010.
- <sup>18</sup>We rewrote the code from scratch in a fully parallel computing structure to exploit the parallel framework of SLEPC and meanwhile be able to incorporate a variety of cluster-impurity model configurations.
- <sup>19</sup>V. I. Anisimov, A. I. Poteryaev, M. A. Korotin, A. O. Anokhin, and G. Kotliar, *J. Phys.: Condens. Matter* **9**, 7359 (1997).
- <sup>20</sup>We adopted the Padé approximant algorithm for numerical analytic continuation (Ref. 21). An effective temperature (Ref. 15) of  $10^{-5}t$  is set for a small  $U$  and  $0.005t$  for a large  $U$ .
- <sup>21</sup>H. J. Vidberg and J. W. Serene, *J. Low Temp. Phys.* **29**, 179 (1977).
- <sup>22</sup>E. H. Lieb and F. Y. Wu, *Phys. Rev. Lett.* **20**, 1445 (1968).
- <sup>23</sup>H. J. Schulz, *Phys. Rev. Lett.* **64**, 2831 (1990).
- <sup>24</sup>C. Honerkamp, *Phys. Rev. Lett.* **100**, 146404 (2008); S. Raghu, X.-L. Qi, C. Honerkamp, and S.-C. Zhang, *ibid.* **100**, 156401 (2008).
- <sup>25</sup>I. F. Herbut, *Phys. Rev. Lett.* **97**, 146401 (2006).
- <sup>26</sup>R.-Q. He and Z.-Y. Lu (unpublished).
- <sup>27</sup>W. F. Brinkman and T. M. Rice, *Phys. Rev. B* **2**, 4302 (1970).